Supplementary Information

Spontaneous interface engineering for dopant-free poly (3-hexylthiophene) perovskite solar cells with efficiency over 24 %

Min Ju Jeong, [a] Kyung Mun Yeom,[a] Se Jin Kim,[a] Eui Hyuk Jung,*[ab] and Jun Hong Noh*[a]

[a] School of Civil, Environmental and Architectural Engineering, Korea University, Seoul 02841, Republic of Korea

[b] Department of Electrical and Computer Engineering, University of Toronto, Toronto, ON M5S 3G4, Canada.

[c] KU-KIST Green School Graduate School of Energy and Environment, Korea University, Seoul 02841, Republic of Korea

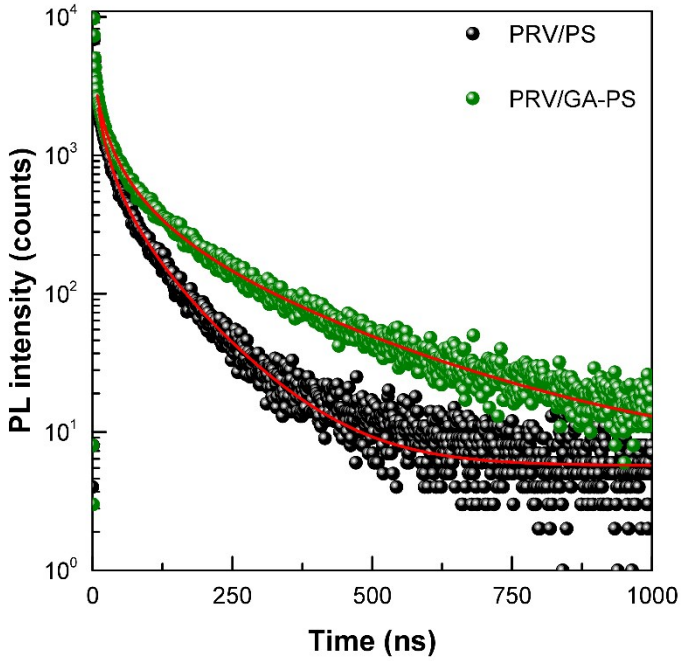

Supplementary Figure 1. TR-PL fitting data excluded initial time decay of (a) PRV/PS and (b) PRV/GA-PS.

The time-dependent charge carrier kinetics can be described by following equation[1]

$$\frac{dn}{dt} = -k_1 n - k_2 n^2 - k_3 n^3 \qquad (1)$$

where n is the charge carrier density, and k_1, k_2, k_3 are the rate constants for first-order (monomolecular), second-order (bimolecular), and third-order (auger) recombination constant, respectively. A single-mode pulsed diode laser (470 nm with a pulse width of ~30 ps, repetition rate of 500 kHz, and an average power of ~50 nW) was used as an excitation source. According to the conditions mentioned above, the TR-PL measurement was conducted at a fluence of 16.4 μJ/cm^2 with 470 nm wavelength (photon fluence: 2.8 x 10^{13} photon/cm^2). The calculated photoexcited carrier density (n_0) by the laser pulse was 6.4 x 10^{17} photon/cm^3, while under the condition auger recombination is negligible. Thus, the first-order and the second-order recombination constants can be calculated by the following equation[2] and the calculated first-order and second-order recombination constants were shown in Supplementary Table 1.

$$n(t) = \frac{k_1 n_0 e^{-k_1 t}}{k_1 + k_2 n_0 \left(1 - e^{-k_1 t}\right)} \qquad (2)$$

where n(t) is time dependent photoexcited charge carrier density, which is proportional the PL decay (PL(t) $\propto$ n(t)). The initial time decay related to the third-order recombination was excluded and the validation of the TR-PL fitting was confirmed via the reduced - Chi square.

Supplementary Table 1. Calculated lifetime and recombination constants fitted from the PL decay of PRV/PS and PRV/GA-PS.

condition	**Lifetime (ns)**	k_1	k_2	**reduced Chi-square**
PRV/PS	108.3	9.23×10^{6}	1.24×10^{-10}	1.16
PRV/GA-PS	298.6	3.35×10^{6}	6.22×10^{-11}	1.10

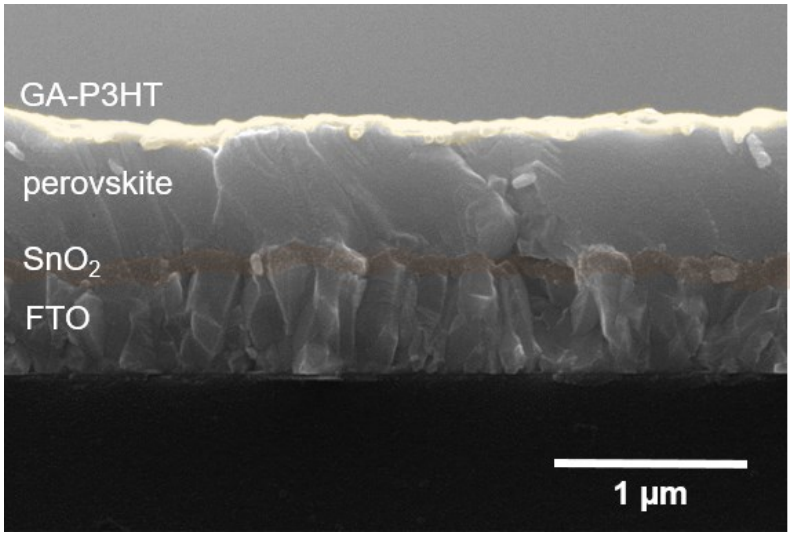

Supplementary Figure 2. The cross-sectional SEM image of the device with FTO/SnO_2/PRV/GA-P3HT structure.

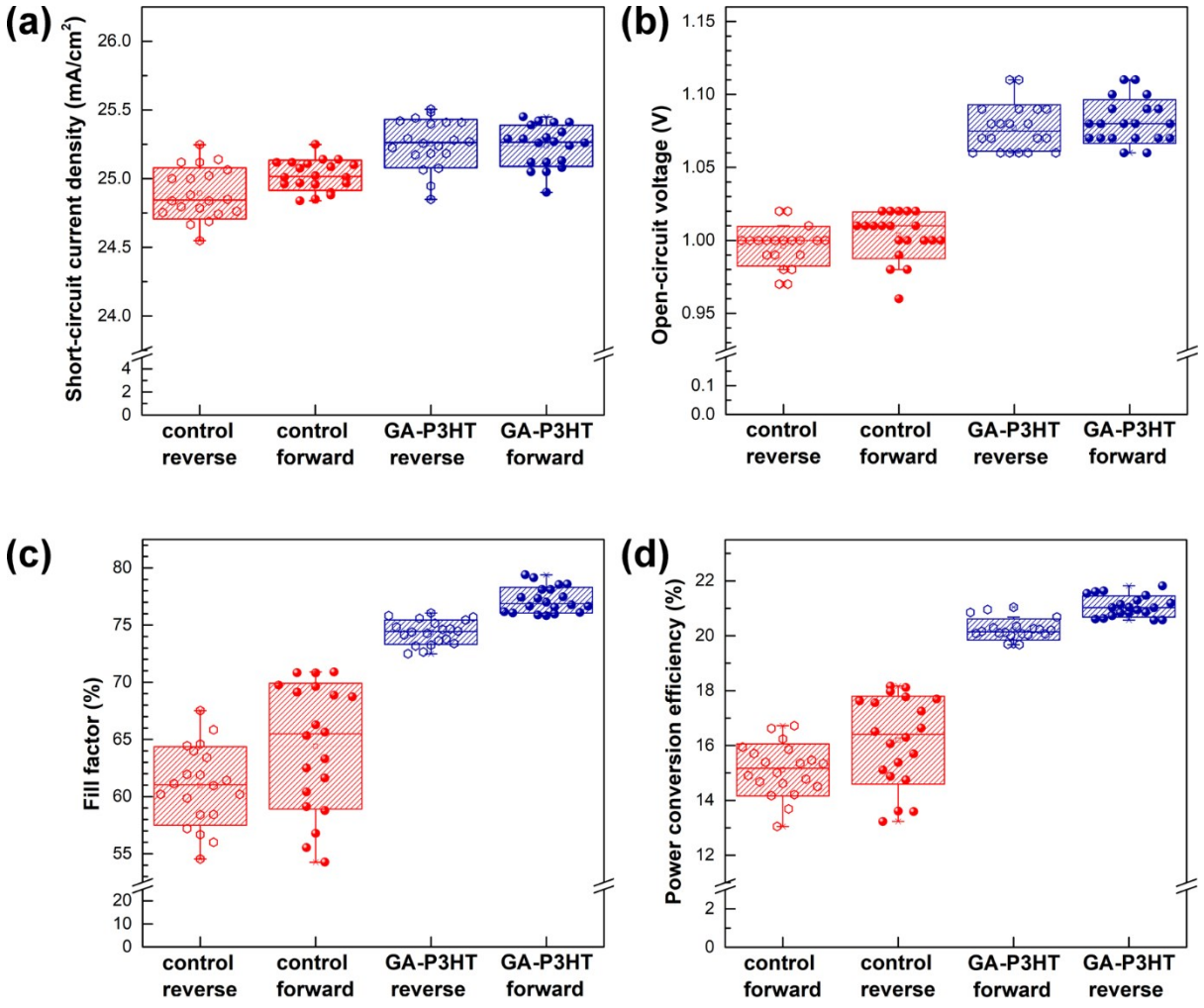

Supplementary Figure 3. Statistics of photovoltaic parameters for 20 PSCs measured along reverse and forward bias scanning direction; (a) Short-circuit current density, (b) open-circuit voltage, (c) fill factor and (d) power conversion efficiency.

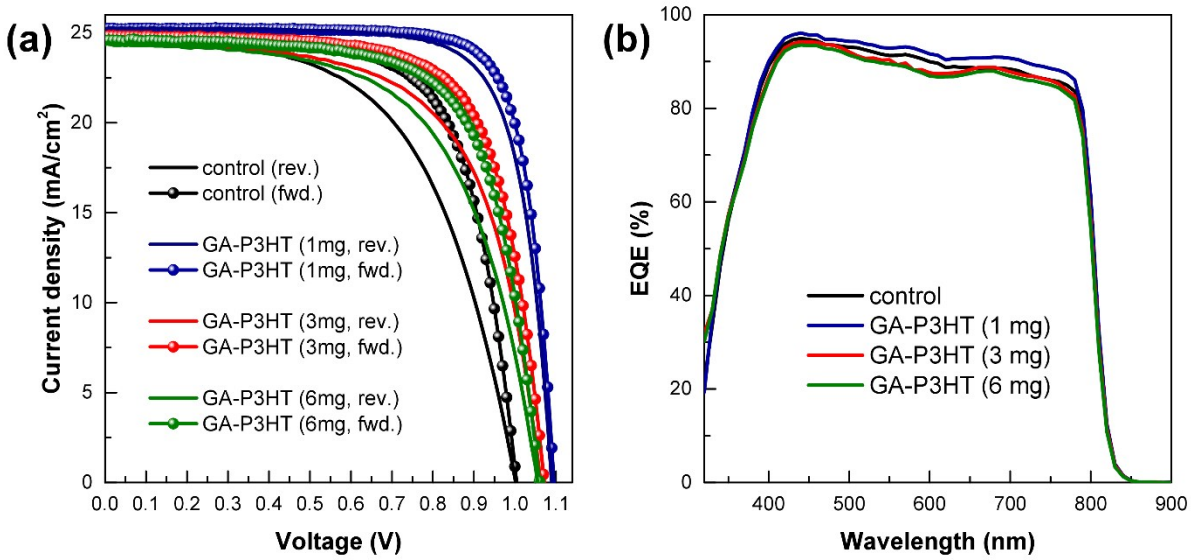

Supplementary Figure 4. (a) *J–V* curves and (b) EQE spectra of perovskite solar cells with pristine P3HT (control), 1, 3, and 6 mg of $Ga(acac)_3$ incorporated P3HT as a hole transport layer, respectively.

Supplementary Table 2. Photovoltaic parameters of perovskite solar cells corresponding with Supplementary Figure 4.

$Ga(acac)_3$ amount†	Scan direction	J_{SC} (mA/cm²)	V_{OC} (V)	FF (%)	PCE (%)	PCE_{avg}*(%)
0 mg	rev.	24.6	1.00	57.2	14.1	15.6
	fwd.	24.8	1.00	69.1	17.1	
1 mg	rev.	25.2	1.09	75.8	20.8	21.3
	fwd.	25.2	1.10	78.6	21.8	
3 mg	rev.	24.5	1.06	63.4	16.5	17.6
	fwd.	24.8	1.07	70.6	18.7	
6 mg	rev.	24.4	1.06	60.4	15.6	16.8
	fwd.	24.6	1.06	69.0	18.0	

† In 1 ml of P3HT solution; * These values were calculated by averaging PCEs obtained from reverse and forward bias scanning.

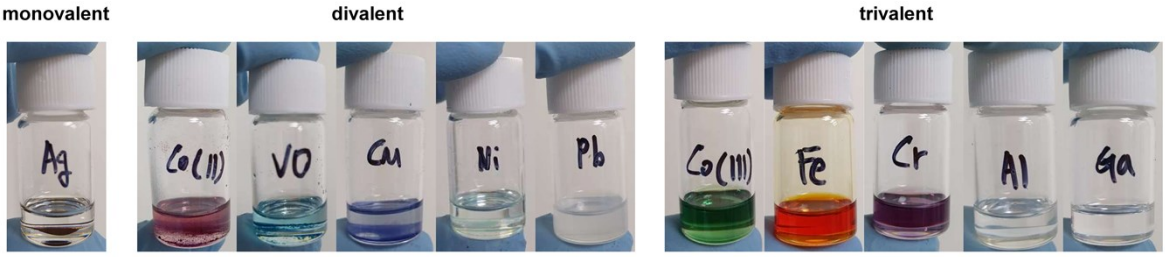

Supplementary Figure 5. The solubility test of monovalent, divalent, and trivalent acetylacetonate in chlorobenzene. All chemicals were mixed with identical molar concentration.

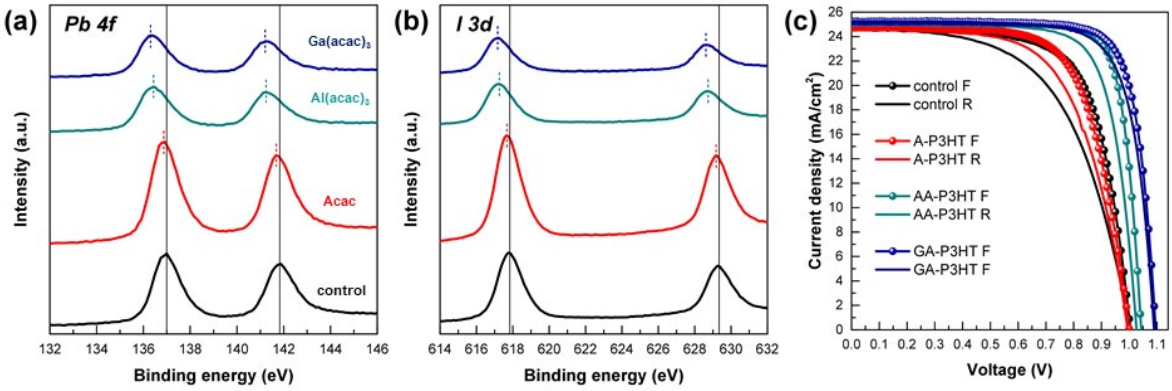

Supplementary Figure 6. X-ray photoelectron spectra of the pristine perovskite and the perovskite films treated by the acetylacetonate (Acac), $Al(acac)_3$, and $Ga(acac)_3$ for (a) Pb 4f, and (b) I 3d signals. (c) *J–V* curves of perovskite solar cells using P3HT incorporated with different metal acetylacetonates (control: pristine P3HT; A-P3HT: P3HT with Acac; AA-P3HT: P3HT with $Al(acac)_3$; GA-P3HT: P3HT with $Ga(acac)_3$).

Supplementary Table 3. Photovoltaic parameters of perovskite solar cells corresponding with Supplementary Figure 6c.

Device	Scan direction	J_{SC} (mA/cm²)	V_{OC} (V)	FF (%)	PCE (%)	PCE_{avg}*(%)
control	rev.	24.6	1.00	57.2	14.1	15.6
	fwd.	24.8	1.00	69.1	17.1	
A-P3HT	rev.	24.6	0.99	63.4	15.4	16.2
	fwd.	24.7	1.00	68.3	16.9	
AA-P3HT	rev.	25.0	1.03	75.0	19.3	20.2
	fwd.	25.1	1.04	81.0	21.1	
GA-P3HT	rev.	25.2	1.09	75.8	20.8	21.3
	fwd.	25.2	1.10	78.6	21.8	

* These values were calculated by averaging PCEs obtained from reverse and forward bias scanning.

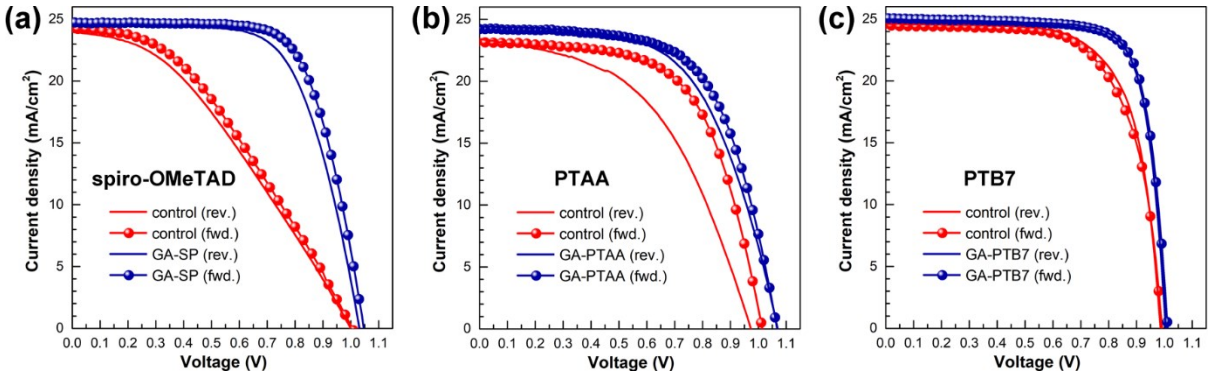

Supplementary Figure 7. Current density-voltage (*J-V*) curves of perovskite solar cells with dopant free (a) spiro-OMeTAD, (b) PTAA and (c) PTB7* hole transport layer.

*PTB7: Poly [[4,8-bis[(2-ethylhexyl)oxy]benzo[1,2-b:4,5-b']dithiophene-2,6-diyl][3-fluoro-2-[(2-ethylhexyl)carbonyl]thieno[3,4-b]thiophenediyl]]

Supplementary Table 4. Photovoltaic characteristics of PSCs with different HTMs.

HTM	$Ga(acac)_3$ addition	Scan direction	J_{SC} (mA/cm²)	V_{OC} (V)	FF (%)	PCE (%)
spiro-OMeTAD	X	rev.	24.0	1.00	36.6	8.8
		fwd.	24.2	1.01	38.1	9.3
	O	rev.	24.5	1.03	65.9	16.6
		fwd.	24.7	1.05	68.9	17.9
PTAA	X	rev.	23.4	0.97	48.7	11.1
		fwd.	23.1	1.01	61.2	14.3
	O	rev.	24.5	1.07	58.4	15.3
		fwd.	24.2	1.07	62.6	16.2
PTB7	X	rev.	24.6	0.99	67.5	16.4
		fwd.	24.4	0.99	69.4	16.8
	O	rev.	25.1	1.01	77.0	19.5
		fwd.	25.0	1.00	78.0	19.5

Supplementary Table 5. TR-PL exponential fit parameter of P3HT and GA-P3HT films on the perovskite film.

condition	A_1	t_1 (ns)	A_2	t_2 (ns)	A_3	t_3 (ns)	t_{avg} (ns)
P3HT	8.4	0.418	0.27	9.6	0.06	53	20
GA-P3HT	54.7	0.352	-	-	-	-	0.352

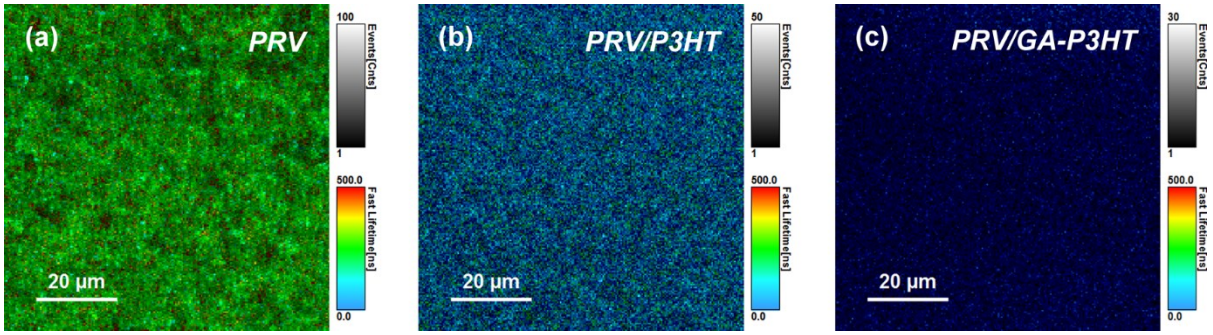

Supplementary Figure 8. 2D carrier lifetime mapping images of (a) perovskite (PRV), (b) perovskite coated with P3HT (PRV/P3HT) and (c) perovskite coated with $Ga(acac)_3$-mixed P3HT (PRV/GA-P3HT).

Supplementary Table 6. Calculated R_{sh}, J_r, and J_d values of control and GA-P3HT devices.

condition	R_{sh} (kΩ cm^2)	J_r (10^{-7} mA/cm^2)	J_d (10^{-9} mA/cm^2)
control	370	4.13	2.05
GA-P3HT	880	3.29	6.87

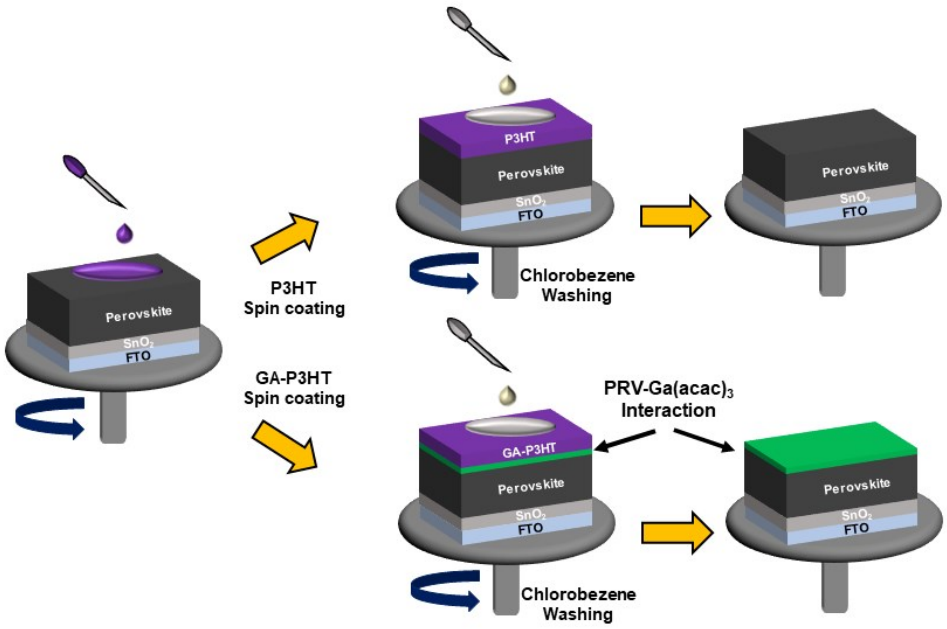

Supplementary Figure 9. Schematic model experimental procedure.

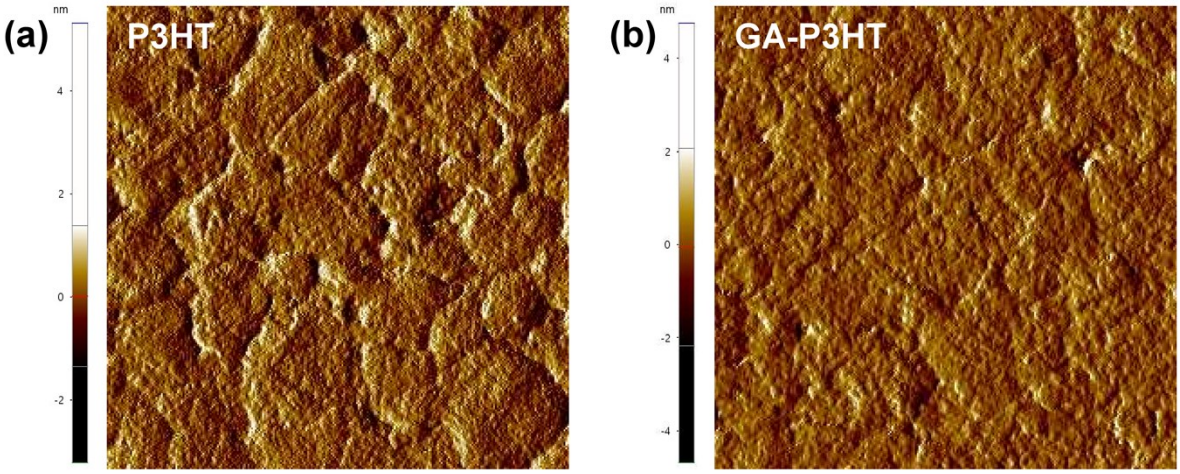

Supplementary Figure 10. AFM images of (a) P3HT (rms: 23.96 nm) and (b) GA-P3HT (rms: 21.68 nm) films on perovskite. The image dimension is 5 μm × 5 μm.

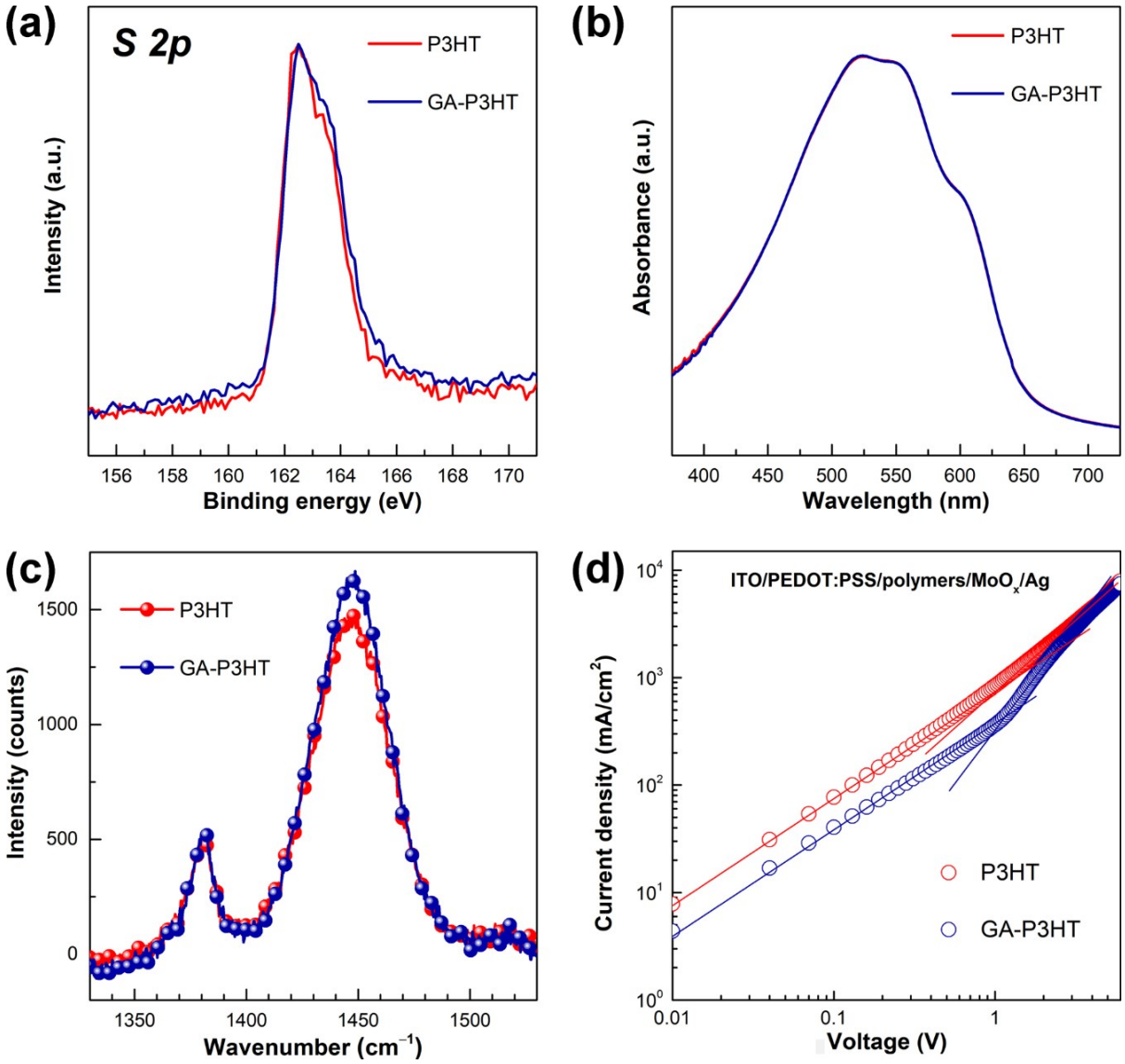

Supplementary Figure 11. (a) X-ray photoelectron spectra of the P3HT and $Ga(acac)_3$-mixed P3HT (GA-P3HT) samples for detecting S 2p signal. (b) UV-visible absorption spectra, (c) Raman spectra of the corresponding samples. (d) *J-V* curves of the hole-only devices with the configuration of ITO/PEDOT:PSS/polymer/MoO_x/Ag. The measurements were performed under dark state.

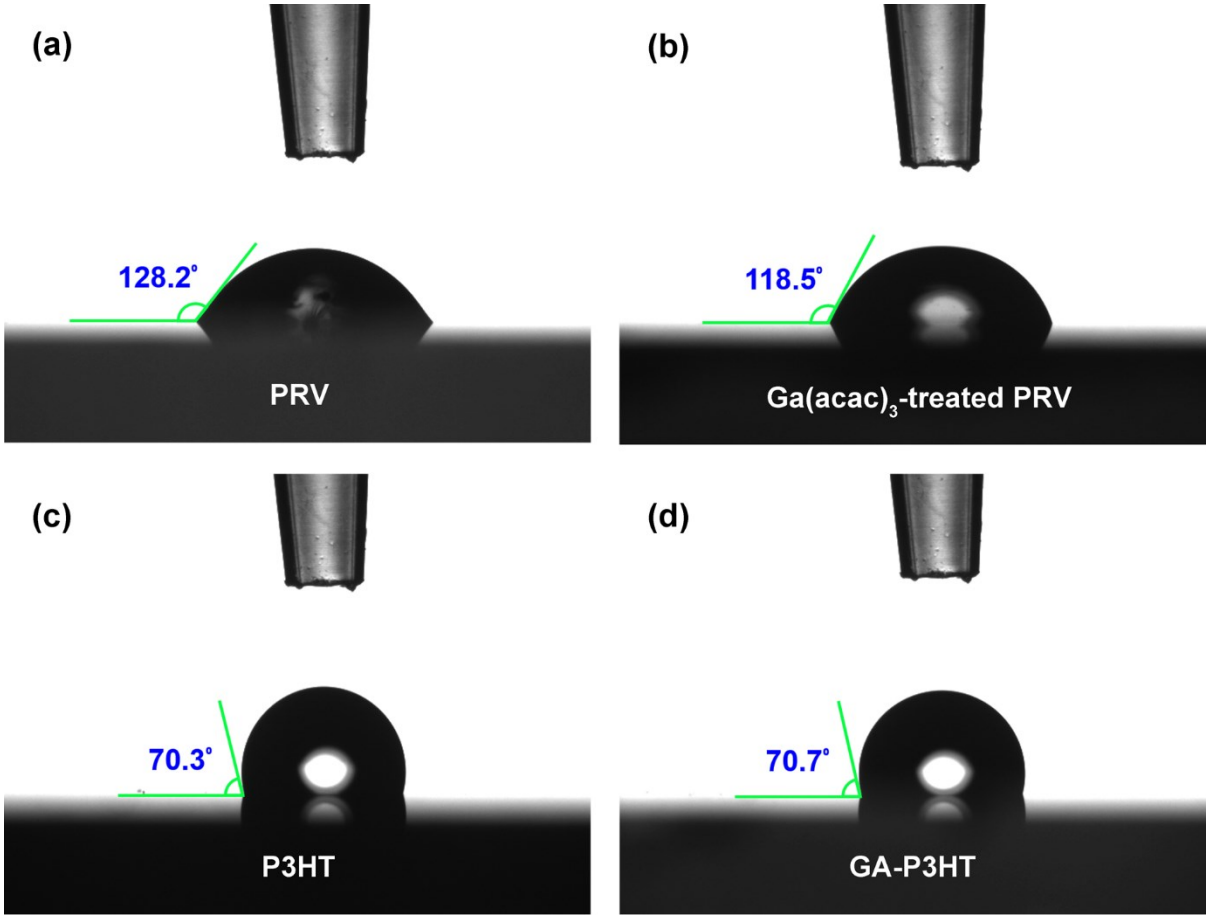

Supplementary Figure 12. Water contact angle images on (a) pristine perovskite (PRV), (b) $Ga(acac)_3$-treated perovskite, (c) pristine P3HT and (d) $Ga(acac)_3$-mixed P3HT. All images were taken 1 second after loading the water droplets.

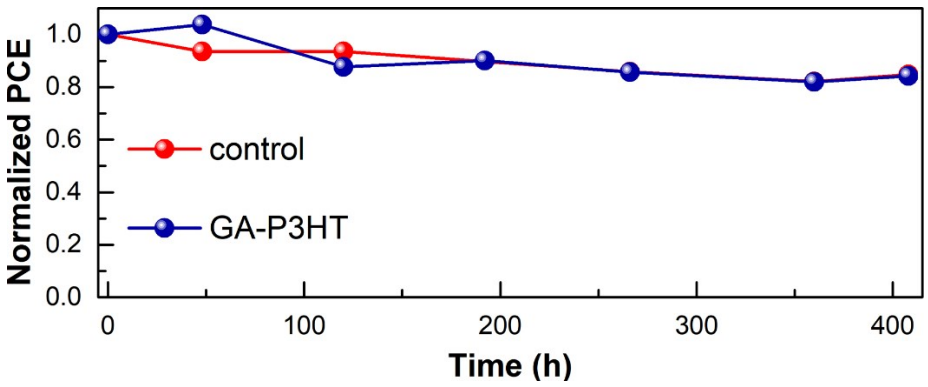

Supplementary Figure 13. PCE evolution of control and GA-P3HT devices under 10% relative humidity at 85℃. The devices were tested without encapsulation.

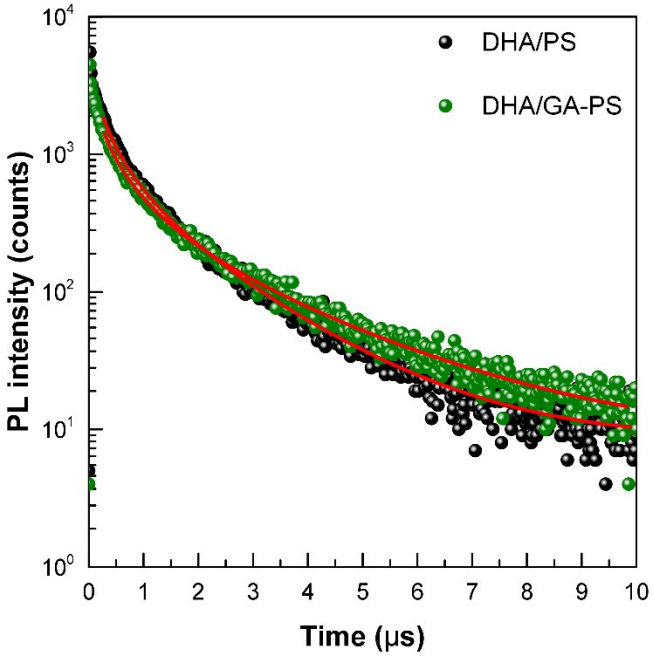

Supplementary Figure 14. TR-PL fitting data excluded initial time decay of (a) DHA/PS and (b) DHA/GA-PS.

Supplementary Table 7. Calculated lifetime and recombination constants fitted from the PL decay of DHA/PS and DHA/GA-PS.

condition	Lifetime (μs)	k_1	k_2	reduced Chi-square
DHA/PS	1.86	5.36×10^{5}	5.32×10^{-12}	1.129
DHA/GA-PS	2.78	3.59×10^{5}	4.86×10^{-12}	1.041

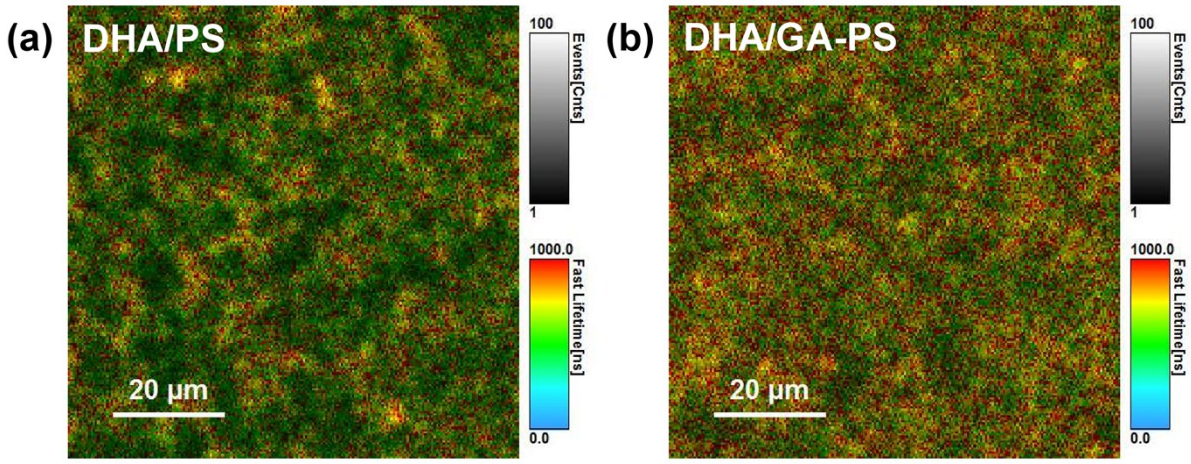

Supplementary Figure 15. 2D carrier lifetime mapping images of (a) DHA/PS and (b) DHA/GA-PS films.

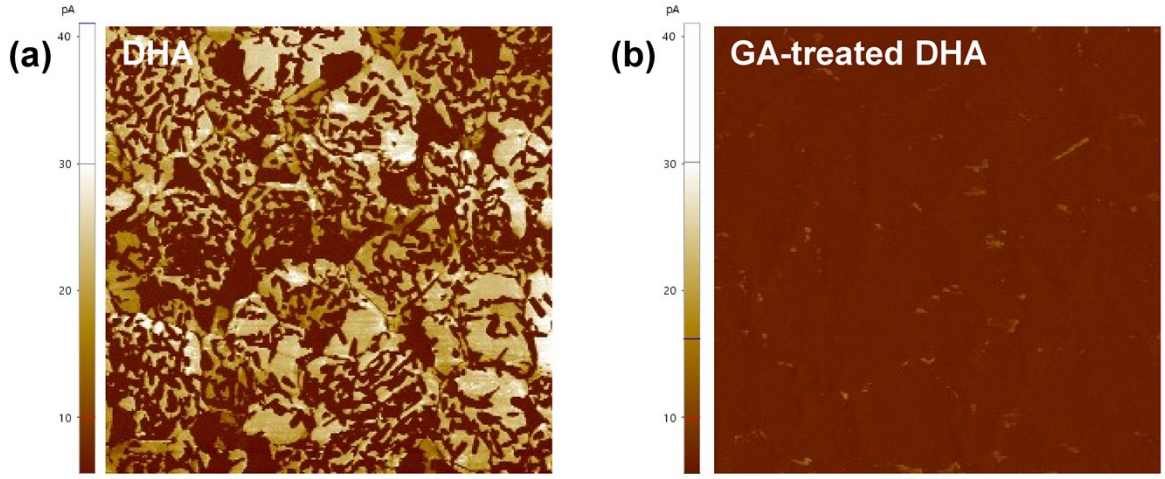

Supplementary Figure 16. Conductive AFM images of DHA and GA-treated DHA film. The image dimension is 5 µm x 5 µm.

Reference

1. J. M. Ball and A. Petrozza, *Nat. Energy*, 2016, **1**, 16149.
2. A. J. Knight, A. D. Wright, J. B. Patel, D. P. McMeekin, H. J. Snaith, M. B. Johnston and L. M. Herz, *ACS Energy Lett.*, 2019, **4**, 75-84.